

Transparent boundary conditions for the sine-Gordon equation: Modeling the reflectionless propagation of kink solitons on a line

K.K. Sabirov^{1,5}, J.R. Yusupov², M. Ehrhardt³ and D.U. Matrasulov⁴

¹*Tashkent University of Information Technologies,
108 Amir Temur Str., 100200, Tashkent Uzbekistan*

²*Yeoju Technical Institute in Tashkent, 156 Usman Nasyr Str., 100121, Tashkent, Uzbekistan*

³*Bergische Universität Wuppertal, Gaußstrasse 20, D-42119 Wuppertal, Germany*

⁴*Turin Polytechnic University in Tashkent, 17 Niyazov Str., 100095, Tashkent, Uzbekistan*

⁵*Tashkent State Technical University named after Islam Karimov,
2 Universitet Str., 100095, Tashkent, Uzbekistan*

We consider the reflectionless transport of sine-Gordon solitons on a line. Transparent boundary conditions for the sine-Gordon equation on a line are derived using the so-called potential approach. Our numerical implementation of these novel boundary conditions proves the absence of the backscattering in transmission of sine-Gordon solitons through the boundary of the considered finite domains.

I. INTRODUCTION

Sine-Gordon solitons are an important class of nonlinear waves appearing in different branches of science and technology, e.g. propagation of fluxons in Josephson junctions in semiconductors, solids, DNA and tectonic plates (see, e.g., the Refs. [1–13], for review). Additionally, the sine-Gordon equation (SGE) appears as the continuous limit of the discrete sine-Gordon equation for the lattice wave field in the Frenkel-Kontorova (FK) model, a model of the dynamic behaviour of crystal defects in solid state. A spatially discrete SGE models the chain of point-like discrete Josephson junctions [14–17]. Each spatial discretization corresponds to a different model.

Unlike other types of nonlinear waves, sine-Gordon solitons are relativistic and, hence, Lorentz invariant waves described by nonlinear partial differential equation involving the d'Alembert operator $\square = \partial_t^2 - \partial_x^2$ (which is invariant under Lorentz transformations) and the sine of the unknown function. A remarkable feature of the sine-Gordon equation on a line is its integrability and the admission of soliton (kink, antikink, breather, etc.) solutions [1, 2]. So far, many aspects of mathematical and physical properties of the sine-Gordon equation and its soliton solutions have been extensively studied, both for traveling and standing waves. Recently, soliton dynamics in networks described in terms of sine-Gordon equation on metric graphs attracted some attention [18–21]. Utilization of such approach makes possible modeling the charged solitons in conducting polymers [22] and static solitons in branched Josephson junctions [23]. However, despite the great progress made on this topic, some issues are still remaining unresolved.

This concerns, e.g., so-called transparent and absorbing boundary conditions for one- and multi-dimensional sine-Gordon equations. Such boundary conditions are determined as those, which make equivalent (similar) the solution of a PDE on a given bounded domain to that in a whole space, so that no back scattering is possible at the boundary for incoming (outgoing) travelling waves. In other words, the wave passing through the boundary does not “feel” it. So far, transparent boundary conditions have been studied for different wave equations having broad applications in physics, such as linear [24–26] and nonlinear [27, 28] Schrödinger, Dirac [29], diffusion [30] and Bogoliubov de Gennes [31] equations. Recently, the concept of transparent boundary conditions have been extended to linear [32–34], nonlinear [35] Schrödinger and Dirac [36] equations on metric graphs.

Until today many different numerical schemes like compact schemes [37–39], predictor-corrector schemes [37, 40], energy-conservative finite difference schemes [41, 42], Lattice-Boltzmann methods [43], radial basis functions [44], etc. were designed to solve numerically the sine-Gordon equation on the real line. The authors simply considered a sufficiently large domain and supplied homogeneous Dirichlet or Neumann boundary condition. Doing so they bypass the main challenge of this problem, namely how to treat appropriately the unbounded domain, since it is not clear what is ‘sufficiently large’ and how does the simple chosen boundary conditions effect the approximation to the whole space solution.

In this paper we address the problem of designing transparent boundary conditions (TBCs) for the 1D sine-Gordon equation using the so-called potential approach previously introduced in [28] (see, also the Refs. [45, 46] for further progress) and utilized in [35] for quantum graphs. Here we will adopt this approach for the sine-Gordon equation on a real line. The motivation for the study of TBCs for the sine-Gordon equation comes from different practical important problems, such as tunable soliton transport in Josephson junctions [7, 23], energy transfer in DNA [12, 13], seismic waves and deformation propagation in tectonic plates [10, 11] and many others. In all these systems for certain cases one needs to achieve reflectionless propagation of waves and particles to avoid different losses in charge, energy and signal transfer. This can be done by imposing TBCs for the governing wave equation and mapping these conditions

on to physical characteristics of the system. Let us note that Zheng [47] presented a different, rather complicated approach for using TBCs for the sine-Gordon equation. Our approach is comparatively simple and more accessible for practitioners.

This paper is organized as follows. In the next section we give details of the procedure for the derivation of transparent boundary conditions for the sine-Gordon equation. Section III presents a prescription for the discretization of these boundary conditions. Section IV provides numerical results for modeling the propagation of sine-Gordon solitons with transparent boundary conditions and the explicit and energy conserving scheme of Fei and Vázquez [42]. Finally, Section V includes some concluding remarks.

II. TRANSPARENT BOUNDARY CONDITIONS FOR THE SINE-GORDON EQUATION

Scattering of nonlinear waves at a given domain's boundary is a problem requiring to use an explicit solution of a wave equation describing these waves. However, the mathematical description of the absence of backscattering is a rather complicated task, since for nonlinear waves there is no S-matrix theory developed in quantum mechanics. Therefore, an effective solution for such problem can be to impose artificial boundary conditions for a wave equation, which describe the reflectionless transmission of the wave through the artificial boundary. TBCs for the evolution equations can be constructed by coupling the solutions of the initial value boundary problems (IVBPs) in the interior and exterior domains [24–26, 48–59].

Briefly, the general procedure for constructing transparent boundary conditions for a given PDE on a real line can be formulated as follows, cf. [48]

1. Splitting the original wave equation into coupled equations, which are determined in the interior and exterior domains on Ω^{int} , Ω^{ext} .
2. Applying a Laplace transformation in time to the exterior problems on Ω^{ext} .
3. Solving the ordinary differential equations in the spatial variable x .
4. Allowing only “outgoing” waves by selecting the asymptotically decaying solution as $x \rightarrow \pm\infty$.
5. Matching the Dirichlet and Neumann values at the artificial boundaries of the interior domain.
6. Applying (numerically) the inverse Laplace transformation.

In this paper, following to the above procedure, we derive transparent boundary conditions for the *sine-Gordon equation* (SGE) on a real line, which reads

$$\partial_x^2 u - \partial_t^2 u - \sin u = 0, \quad x \in \mathbb{R}, t > 0, \quad (1)$$

and is supplied with the following initial conditions:

$$u(x, 0) = u_0(x), \quad \partial_t u(x, 0) = u_1(x). \quad (2)$$

Let us note that Eq. (1) admits a *soliton solution* in the form of a kink given by

$$u(x, t) = 4 \tan^{-1} \exp \left[\pm \frac{x - x_0 - vt}{\sqrt{1 - v^2}} \right], \quad (3)$$

where v denotes the (constant) velocity of the kink. For completeness, we add (e.g., from [3]) other solutions:

$$\text{Breather: } u(x, t) = 4 \tan^{-1} \left[\frac{\sqrt{1 - v^2}}{v} \frac{\sin(v(t - t_0))}{\cosh(\sqrt{1 - v^2}(x - x_0))} \right], \quad (4)$$

$$\text{Kink-Antikink: } u(x, t) = 4 \tan^{-1} \left[\frac{v \cosh((x - x_0)/\sqrt{1 - v^2})}{\sinh(vt/\sqrt{1 - v^2})} \right]. \quad (5)$$

Furthermore, it is well-known [42] that the solutions to (1) conserve the *total energy* (sum of kinetic, strain and potential energies)

$$E = \int_{\mathbb{R}} \left[\frac{1}{2} (\partial_t u(x, t))^2 + \frac{1}{2} (\partial_x u(x, t))^2 + G(u(x, t)) \right] dx = \text{const.} \quad (6)$$

with the *potential function* $G(u) = 1 - \cos u$, e.g. the kink (3) has the energy $8/\sqrt{1-v^2}$, and the momentum

$$P = - \int_{\mathbb{R}} (\partial_t u)(\partial_t u) dx = \frac{8v}{\sqrt{1-v^2}}, \quad (7)$$

cf. [42]. These invariants (or their discrete versions) can be used later to check the usability of the considered numerical scheme.

Here we consider the propagation of a sine-Gordon soliton given by Eq. (3) on a finite interval $[0, L]$ and require its reflectionless transmission through the boundary of the interval, at $x = 0$ and $x = L$ in terms of the boundary conditions for Eq. (1).

For this purpose we apply the so-called *potential approach*, which was earlier applied for the derivation of TBCs for the nonlinear Schrödinger equation [27]. Within such an approach, one reduces the sine-Gordon equation (1) into a linear PDE by introducing the following potential:

$$V(x, t) = - \frac{\sin u(x, t)}{u(x, t)}. \quad (8)$$

It should be noted that this potential approach neglects here the dependency on the solution u and considers it again at a later step. Doing so, one can formally rewrite Eq. (1) as the *linear Klein-Gordon equation*

$$\partial_x^2 u - \partial_t^2 u + V(x, t)u = 0, \quad 0 < x < L, \quad t > 0. \quad (9)$$

Next, introducing the new (unknown) function v , defined by the $v(x, t) = e^{-\nu(x, t)}u(x, t)$, where

$$\nu(x, t) = \int_0^t \int_0^\tau V(x, s) ds d\tau, \quad (10)$$

we obtain the following relations for the time and space derivatives of u :

$$\begin{aligned} \partial_t u &= e^\nu (\partial_t \nu + \partial_t) v, \\ \partial_t^2 u &= e^\nu [(\partial_t \nu)^2 + 2\partial_t \nu \cdot \partial_t + \partial_t^2 + V] v, \end{aligned}$$

and

$$\begin{aligned} \partial_x u &= e^\nu (\partial_x \nu + \partial_x) v, \\ \partial_x^2 u &= e^\nu [(\partial_x \nu)^2 + 2\partial_x \nu \cdot \partial_x + \partial_x^2 + \partial_x^2 \nu] v. \end{aligned}$$

Then, the left hand side of Eq. (9) for the new variable v reads

$$\mathcal{L}(x, t, \partial_x, \partial_t)v = \partial_x^2 v - \partial_t^2 v + A\partial_x v + (B - C)v - D\partial_t v, \quad (11)$$

where we have introduced the abbreviations

$$A = 2\partial_x \nu, \quad B = \partial_x^2 \nu + (\partial_x \nu)^2, \quad C = (\partial_t \nu)^2, \quad D = 2\partial_t \nu.$$

The operator \mathcal{L} in Eq. (11) can be formally factorized as

$$\mathcal{L} = (\partial_x - \Lambda^-)(\partial_x + \Lambda^+) = \partial_x^2 + (\Lambda^+ - \Lambda^-)\partial_x + \text{Op}(\partial_x \lambda^+) - \Lambda^- \Lambda^+. \quad (12)$$

Furthermore, we introduce the system of pseudo differential operators [60] and comparing with (11) leads to

$$\begin{aligned} \Lambda^+ - \Lambda^- &= A, \\ \text{Op}(\partial_x \lambda^+) - \Lambda^- \Lambda^+ &= -\partial_t^2 - D\partial_t + B - C, \end{aligned} \quad (13)$$

which yields the following system of equations on the symbol level:

$$\begin{aligned} \lambda^+ - \lambda^- &= a, \\ \partial_x \lambda^+ - \sum_{\alpha=0}^{+\infty} \frac{1}{\alpha!} \partial_\tau^\alpha \lambda^- \partial_t^\alpha \lambda^+ &= -\tau^2 - d\tau + b - c, \end{aligned} \quad (14)$$

where we have set $a = A$, $b = B$, $c = C$, $d = D$. The total symbol λ^\pm of the pseudo differential operator Λ^\pm admits an asymptotic expansion in inhomogeneous symbols as

$$\lambda^\pm \sim \sum_{j=0}^{+\infty} \lambda_{1-j}^\pm. \quad (15)$$

If one considers only first order terms, then from the first equation one obtains $\lambda_1^- = \lambda_1^+$. Accordingly, from the second equation of the system (14) we have

$$\lambda_1^+ = \pm \tau. \quad (16)$$

For the potential $V(x, t)$, the Dirichlet-to-Neumann (DtN) formulation of the TBC corresponds to the choice $\lambda_1^+ = \tau$. For the zero order terms we get

$$\begin{aligned} \lambda_0^+ - \lambda_0^- &= a, \\ \partial_x \lambda_1^+ - (\lambda_1^- \lambda_0^+ + \lambda_0^- \lambda_1^+) &= -d\tau, \quad \text{i.e.} \quad \partial_x \lambda_1^+ - (\lambda_0^+ + \lambda_0^-)\tau = -d\tau. \end{aligned} \quad (17)$$

Using $\partial_x \lambda_1^+ = 0$ from (17) we have

$$\lambda_0^+ = \frac{a}{2} + \frac{d}{2} = \partial_x \nu + \partial_t \nu, \quad \lambda_0^- = -\frac{a}{2} + \frac{d}{2} = -\partial_x \nu + \partial_t \nu. \quad (18)$$

For $j = 2$ we have

$$\begin{aligned} \lambda_{-1}^+ - \lambda_{-1}^- &= 0, \\ \partial_x \lambda_0^+ - (\lambda_1^- \lambda_{-1}^+ + \lambda_0^- \lambda_0^+ + \lambda_{-1}^- \lambda_1^+ + \partial_\tau \lambda_1^- \partial_t \lambda_0^+ + \partial_\tau \lambda_1^- \partial_t \lambda_{-1}^+) &= b - c, \end{aligned} \quad (19)$$

since $\partial_\tau^\alpha \lambda_0^\pm = 0$, $\partial_t^\alpha \lambda_1^\pm = 0$, $\alpha \in N$ and $\partial_\tau^\beta \lambda_1^\pm = 0$, $\beta \in \{2, 3, 4, \dots\}$. Now using (18) the second equation simplifies to

$$\begin{aligned} \partial_t \lambda_{-1}^\pm + 2\lambda_{-1}^\pm \tau &= \partial_x \lambda_0^+ - \partial_t \lambda_0^+ - \partial_x^2 \nu \\ &= -\partial_{tt}^2 \nu. \end{aligned}$$

From the last equation we obtain finally

$$\lambda_{-1}^- = \lambda_{-1}^+ = -\int_0^t V(x, s) \cdot e^{-2\tau(t-s)} ds. \quad (20)$$

This procedure can be continued for $j > 2$. Now the DtN TBC applied to the function v can be written as

$$(\partial_x \pm \Lambda^\pm)v = 0, \quad (21)$$

or equivalently

$$(\partial_x \pm \Lambda^\pm)e^{-\nu}u = 0. \quad (22)$$

Following the Refs. [27, 28], we apply a ‘‘cut-off’’ (up to $M - 1$ th term) in the expansion Λ as

$$\Lambda_M^\pm = \text{Op} \left(\sum_{j=0}^{M-1} \lambda_{1-j}^\pm \right). \quad (23)$$

In this paper, we restrict ourselves to considering the expansion in Eq. (23) up to the third order approximation for transparent boundary conditions. Using (16), (18) and (20), we obtain

$$\begin{aligned} \Lambda_1^\pm f &= \partial_t f, \\ \Lambda_2^\pm f &= \partial_t f \pm \partial_x \nu \cdot f + \partial_t \nu \cdot f, \\ \Lambda_3^\pm f &= \partial_t f \pm \partial_x \nu \cdot f + \partial_t \nu \cdot f - e^{-2} \partial_t \nu \cdot f. \end{aligned}$$

These results yield to the following TBCs.

The first order approximation.

For the left boundary (at $x = 0$) we obtain the following expression:

$$\partial_x u(0, t) = \left[\partial_t u(x, t) + \left(\partial_x \nu(x, t) - \partial_t \nu(x, t) \right) \cdot u(x, t) \right]_{x=0}, \quad (24)$$

Analogously, one can obtain the TBC for the right boundary (at $x = L$):

$$\partial_x u(L, t) = \left[-\partial_t u(x, t) + \left(\partial_x \nu(x, t) + \partial_t \nu(x, t) \right) \cdot u(x, t) \right]_{x=L}. \quad (25)$$

The second order approximation.

For the left boundary (at $x = 0$):

$$\partial_x u(0, t) = \partial_t u(0, t), \quad (26)$$

and for the right boundary (at $x = L$):

$$\partial_x u(L, t) = -\partial_t u(L, t). \quad (27)$$

The third order approximation.

For the left boundary (at $x = 0$):

$$\partial_x u(0, t) = \left[\partial_t u(x, t) - e^{-2} \cdot \partial_t \nu(x, t) \cdot u(x, t) \right]_{x=0}. \quad (28)$$

and for the right boundary (at $x = L$):

$$\partial_x u(L, t) = \left[-\partial_t u(x, t) + e^{-2} \cdot \partial_t \nu(x, t) \cdot u(x, t) \right]_{x=L}. \quad (29)$$

Eqs. (24)-(29) represent approximations to the transparent boundary conditions for the sine-Gordon equation (1), which provide reflectionless transport of the sine-Gordon solitons on a real line. It remains to implement these approximations in a numerical scheme, which is a non-trivial task since these TBCs are nonlocal in time (of memory-type) with a singular kernel.

III. DISCRETIZATION SINE-GORDON EQUATION AND TRANSPARENT BOUNDARY CONDITIONS

The efficient numerical implementation of the above transparent boundary conditions (24)–(29) is a non-trivial task and requires using highly accurate and stable discretization schemes. We introduce the notation $k = \Delta t$, $h = \Delta x$, and D_k^+ , D_k^- , D_k^0 , $D_k^2 = D_k^+ D_k^-$ are the standard (forward, backward, centered, second order) difference quotients with step sizes in time k or space h . Further, (\cdot, \cdot) denotes the standard inner product on the real line, i.e.

$$(u^n, v^n) = h \sum_{j \in \mathbb{Z}} u_j^n v_j^n, \quad (30)$$

inducing the norm $\|u^n\|^2 = (u^n, u^n)$ and the semi-norm

$$|u^n|_1^2 = \frac{1}{2} \|D_h^+ u^n\|^2 + \frac{1}{2} \|D_h^- u^n\|^2. \quad (31)$$

A. The standard discretization

Let us recall that the standard discretization for the sine-Gordon equation (1) uses central second difference quotients for approximating $\partial_t^2 u$, $\partial_x^2 u$ and reads

$$\frac{u_j^{n+2} - 2u_j^{n+1} + u_j^n}{\Delta t^2} - \frac{u_{j+1}^{n+1} - 2u_j^{n+1} + u_{j-1}^{n+1}}{\Delta x^2} + \sin(u_j^{n+1}) = 0, \quad j \in \mathbb{Z}, n \geq 0. \quad (32)$$

i.e. in our notation

$$D_k^2 u_j^{n+1} - D_h^2 u_j^{n+1} + \sin(u_j^{n+1}) = 0, \quad j \in \mathbb{Z}, n \geq 0. \quad (33)$$

This leads to the following explicit scheme

$$u_j^{n+2} = 2(1 - \gamma^2)u_j^{n+1} + \gamma^2(u_{j+1}^{n+1} + u_{j-1}^{n+1}) - \Delta t^2 \sin(u_j^{n+1}) - u_j^n, \quad j \in \mathbb{Z}, n \geq 0, \quad (34)$$

where $\gamma = \Delta t / \Delta x$ denotes the hyperbolic mesh ratio. For the starting step ($n = -1$) we use the central difference with the ghost value u_j^{-1}

$$\partial_t u(x_j, 0) = u_1(x_j) = \frac{u_j^1 - u_j^{-1}}{2\Delta t} + O(\Delta t^2)$$

and obtain from (34)

$$u_j^1 = \Delta t u_1(x_j) + (1 - \gamma^2)u_j^0 + \frac{\gamma^2}{2}(u_{j+1}^0 + u_{j-1}^0) - \frac{\Delta t^2}{2} \sin(u_j^0), \quad (35)$$

with the initial data $u_j^0 = u_0(x_j)$, $j = 0, 1, \dots, J$.

For checking the discrete energy conservation (and thus the stability and the suitability to model the long time behavior of the solution) we multiply (33) with the central difference quotient $D_k^0 u_j^{n+1} = (u_j^{n+2} - u_j^n) / (2k)$ and obtain

$$\frac{1}{2} D_k^- (D_k^+ u_j^{n+1})^2 - (D_k^0 u_j^{n+1}) (D_h^- D_h^+ u_j^{n+1}) + (D_k^0 u_j^{n+1}) \sin(u_j^{n+1}) = 0, \quad j \in \mathbb{Z}, n \geq 0. \quad (36)$$

Next, summing over $j \in \mathbb{Z}$ and summation by parts yields

$$D_k^- \sum_{j \in \mathbb{Z}} \frac{1}{2} (D_k^+ u_j^{n+1})^2 + \sum_{j \in \mathbb{Z}} (D_k^0 D_h^+ u_j^{n+1}) (D_h^+ u_j^{n+1}) + \sum_{j \in \mathbb{Z}} (D_k^0 u_j^{n+1}) \sin(u_j^{n+1}) = 0, \quad n \geq 0. \quad (37)$$

B. An explicit energy conserving scheme

The third term in (37) arising from the standard discretization prevents a proper energy conservation and for this reason we modify the sine term in the scheme:

$$\frac{u_j^{n+2} - 2u_j^{n+1} + u_j^n}{\Delta t^2} - \frac{u_{j+1}^{n+1} - 2u_j^{n+1} + u_{j-1}^{n+1}}{\Delta x^2} = \frac{\cos(u_j^{n+2}) - \cos(u_j^n)}{u_j^{n+2} - u_j^n}, \quad j \in \mathbb{Z}, n \geq 0. \quad (38)$$

The right hand side of Eq. (38) is a second order approximation to $-\sin(u_j^{n+1})$ which explains the consistency to (1).

It can be shown using the same steps as in (36), (37) that this implicit scheme (38) satisfies on $j \in \mathbb{Z}$ a discrete analogue of the energy conservation (6), cf. [42]

$$E_0^{n+1} = h \sum_{j \in \mathbb{Z}} \left[\frac{1}{2} (D_k^+ u_j^n)^2 + \frac{1}{2} (D_h^+ u_j^{n+1}) (D_h^+ u_j^n) + \frac{G(u_j^{n+1}) + G(u_j^n)}{2} \right] = \text{const.} \quad (39)$$

Additionally, we modify the temporal discretization in Eq. (38) to obtain an efficient explicit scheme:

$$\frac{u_j^{n+3} - (u_j^{n+2} + u_j^{n+1}) + u_j^n}{2\Delta t^2} - \frac{u_{j+1}^{n+2} - 2u_j^{n+2} + u_{j-1}^{n+2}}{\Delta x^2} - \frac{u_{j+1}^{n+1} - 2u_j^{n+1} + u_{j-1}^{n+1}}{\Delta x^2} = \frac{\cos(u_j^{n+2}) - \cos(u_j^{n+1})}{u_j^{n+2} - u_j^{n+1}}, \quad (40)$$

$j \in \mathbb{Z}$, $n \geq 0$, which was proposed by Fei and Vazquez [42] as ‘Scheme 1 (S1)’ and reads in our notation

$$D_k^2 u_j^{n+3/2} - D_h^2 u_j^{n+3/2} + \frac{G(u_j^{n+2}) - G(u_j^{n+1})}{u_j^{n+2} - u_j^{n+1}} = 0, \quad j \in \mathbb{Z}, n \geq 0. \quad (41)$$

Here, we have introduced the arithmetic averaging $u_j^{n+3/2} = (u_j^{n+2} + u_j^{n+1})/2$. The solution u_j^{n+3} can be computed explicitly from the difference equation (40), once the starting values u_j^0, u_j^1, u_j^2 are available. Also, the scheme (40) is second order in time and space and fulfills for $j \in \mathbb{Z}$ the discrete energy conservation, cf. [42]

$$E_1^{n+1} = h \sum_{j \in \mathbb{Z}} \left[\frac{1}{2} (D_k^+ u_j^{n+1}) (D_k^- u_j^{n+1}) + \frac{1}{2} (D_h^+ u_j^{n+1})^2 + G(u_j^{n+1}) \right] = \text{const}. \quad (42)$$

Let us note that Vu-Quoc and Li [61, 62] investigated the construction of energy conserving finite difference schemes for nonlinear Klein-Gordon equations in a general setting.

C. Implementation of the TBC

In this subsection we present our numerical method for finding values of the wave function at transparent boundaries. Here we give prescription only for the TBC of the third approximation (29) at $x = L$. We note that for the first and second approximations the implementation can be done analogously. Thus, denoting $g = u_j^n$, in each time step one needs to find zero of the following function

$$f(g) = \gamma (g - u_{j-1}^n) + (g - u_{j-1}^n) - \Delta t e^{-2} \partial_t \nu^n(g) \cdot g. \quad (43)$$

The function zeros can be found using the Newton-Raphson method, for which the derivative of the function is required:

$$f'(g) = \gamma + 1 - \Delta t e^{-2} \left([\partial_t \nu^n(g)]' \cdot g + \partial_t \nu^n(g) \right). \quad (44)$$

We discretize the double integral function $\nu(x, t) \approx \nu^n(x)$ given by (10) using the trapezoidal rule in the following way

$$\begin{aligned} \nu^n(x) &= \nu^{n-1}(x) + \int_{t_{n-1}}^{t_n} \int_0^\tau V(x, s) ds d\tau = \nu^{n-1}(x) + \frac{\Delta t}{2} \left(\int_0^{t_{n-1}} V(x, s) ds + \int_0^{t_n} V(x, s) ds \right) \\ &= \nu^{n-1}(x) + \frac{\Delta t}{2} \left[\frac{\Delta t}{2} \left(V^0(x) + 2 \sum_{k=1}^{n-2} V^k(x) + V^{n-1}(x) \right) + \frac{\Delta t}{2} \left(V^0(x) + 2 \sum_{k=1}^{n-1} V^k(x) + V^n(x) \right) \right] \\ &= \nu^{n-1}(x) + \frac{\Delta t^2}{4} \left(2V^0(x) + 4 \sum_{k=1}^{n-2} V^k(x) + 3V^{n-1}(x) + V^n(x) \right), \quad n \geq 2, \end{aligned}$$

where $\nu^0(x) = 0$ and $\nu^1(x) = \frac{\Delta t^2}{4} (V^0(x) + V^1(x))$.

In the same way one can discretize

$$\partial_t \nu(x, t) = \int_0^t V(x, s) ds$$

using the same trapezoidal rule as

$$\partial_t \nu(x, t) \approx \partial_t \nu^n(x) = \frac{\Delta t}{2} \left(V^0(x) + 2 \sum_{k=1}^{n-1} V^k(x) + V^n(x) \right).$$

Similarly, $\partial_x \nu(x, t)$ (which is needed in the first order approximation) can be approximated as follows

$$\partial_x \nu(x, t) = \int_0^t \int_0^\xi \partial_x V(x, s) ds d\xi \approx \partial_x \nu^n(x),$$

where

$$\partial_x \nu^n(x) = \partial_x \nu^{n-1}(x) + \frac{\Delta t^2}{4} \left(2\partial_x V^0(x) + 4 \sum_{k=1}^{n-2} \partial_x V^k(x) + 3\partial_x V^{n-1}(x) + \partial_x V^n(x) \right)$$

$$\text{with } \partial_x V^k(x_j) = \partial_g \left(-\frac{\sin g}{g} \right) \Big|_{g=u_j^k} \cdot \frac{u_j^k - u_{j-1}^k}{\Delta x}.$$

For the derivative in (44) one can use the following approximation

$$[\partial_t \nu^n(g)]' = \frac{\Delta t}{4} F'(g), \quad n \geq 1,$$

with $[\partial_t \nu^0(g)]' = 0$.

In the next section, where we present a numerical example, we use this prescription in our numerical calculations of TBCs.

D. Stability of the overall scheme

It remains to check the stability of the scheme (41) on a bounded grid supplied with our discretized TBC at $x = 0$, $x = L$ (i.e. $j = 0$, $j = J$). Thus we have to consider the inner product (\cdot, \cdot) on a finite range $j = 0, 1, \dots, J$

$$(u^n, v^n)_J = h \sum_{j=1}^{J-1} u_j^n v_j^n, \quad (45)$$

with the corresponding induced norms and semi-norms as in (31). Next, we multiply (41) by $D_{k/2}^0 u_j^{n+3/2} = D_k^+ u_j^{n+1} = (u_j^{n+2} - u_j^{n+1})/k$ and take the inner product (45)

$$h \sum_{j=1}^{J-1} D_k^+ u_j^{n+1} D_k^2 u_j^{n+3/2} - h \sum_{j=1}^{J-1} D_k^+ u_j^{n+1} D_h^2 u_j^{n+3/2} + \frac{h}{k} \sum_{j=1}^{J-1} (G(u_j^{n+2}) - G(u_j^{n+1})) = 0, \quad j \in \mathbb{Z}, \quad n \geq 0. \quad (46)$$

An easy calculation proves the following identity for the first term, cf. (42)

$$D_k^+ u_j^{n+1} D_k^2 u_j^{n+3/2} = D_k^+ \frac{1}{2} (D_k^+ u_j^{n+1}) (D_k^- u_j^{n+1}). \quad (47)$$

Then we apply the summation by parts rule for two grid functions f_j, g_j on a finite index range

$$h \sum_{j=1}^{J-1} g_j D_h^- f_j = -h \sum_{j=0}^{J-1} f_j D_h^+ g_j + f_{J-1} g_J - f_0 g_0 \quad (48)$$

and obtain choosing $g_j = D_k^+ u_j^{n+1}$, $f_j = D_h^+ u_j^{n+3/2}$

$$\begin{aligned} D_k^+ h \sum_{j=1}^{J-1} \frac{1}{2} (D_k^+ u_j^{n+1}) (D_k^- u_j^{n+1}) + h \sum_{j=0}^{J-1} (D_h^+ u_j^{n+3/2}) D_h^+ (D_k^+ u_j^{n+1}) + D_k^+ h \sum_{j=1}^{J-1} G(u_j^{n+1}) \\ = (D_h^- u_J^{n+3/2}) (D_k^+ u_J^{n+1}) - (D_h^+ u_0^{n+3/2}) (D_k^+ u_0^{n+1}), \quad n \geq 0. \end{aligned} \quad (49)$$

Another elementary algebraic calculation shows for the second term, cf. (42)

$$(D_h^+ u_j^{n+3/2}) D_h^+ (D_k^+ u_j^{n+1}) = D_k^+ \frac{1}{2} (D_h^+ u_j^{n+1})^2, \quad (50)$$

i.e. we obtain

$$\begin{aligned} D_k^+ h \sum_{j=1}^{J-1} \left[\frac{1}{2} (D_k^+ u_j^{n+1}) (D_k^- u_j^{n+1}) + \frac{1}{2} (D_h^+ u_j^{n+1})^2 + G(u_j^{n+1}) \right] \\ = (D_h^- u_J^{n+3/2}) (D_k^+ u_J^{n+1}) - (D_h^+ u_0^{n+3/2}) (D_k^+ u_0^{n+1}), \quad n \geq 0. \end{aligned} \quad (51)$$

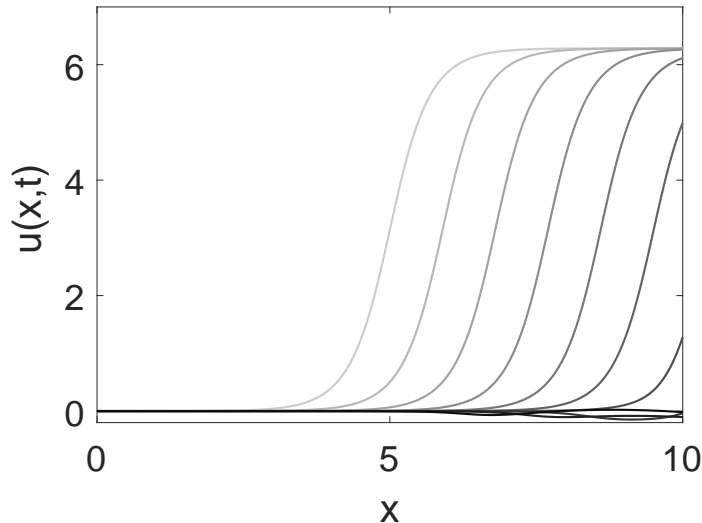


FIG. 1: Evolution of a kink (53) simulated with finite difference scheme given by (38). This plot is obtained for TBC of the third order approximation (29).

The left hand side of (51) is exactly the discrete time derivative $D_k^+ E_1^{n+1}$ of the discrete energy defined in (42), i.e. for a stable overall scheme one has to check finally (possibly only numerically for nonstandard boundary conditions like the TBCs) if the right hand side of (51) (the boundary terms) are negative, such that the discrete energy will decay on the finite interval. E.g. in the simple cases of Dirichlet boundary conditions we have $D_k^+ u_0^{n+1} = 0$, $D_k^+ u_J^{n+1} = 0$ and for homogeneous Neumann boundary conditions the discrete normal derivatives $D_h^+ u_0^{n+3/2}$, $D_h^+ u_J^{n+3/2}$ vanish, i.e., for these standard boundary conditions the right hand side of (51) is zero, the discrete energy E_1^{n+1} is conserved and thus the overall scheme is stable.

Analogously one can check the sign of the boundary terms in (51) for the TBCs, e.g. the second order approximation (26), (27) is discretized as follows

$$D_h^+ u_0^{n+3/2} = D_k^+ u_0^{n+1}, \quad D_h^+ u_J^{n+3/2} = -D_k^+ u_J^{n+1} \quad (52)$$

and thus the right hand side of (51) is negative, i.e. the discrete energy E_1^{n+1} decays and thus the overall scheme is stable.

IV. NUMERICAL EXAMPLE

Now we solve the sine-Gordon equation (1) on the finite interval $[0, L]$ imposing TBC at the right boundary (i.e. at $x = L$). As the initial conditions we choose a kink-soliton at $t = 0$

$$u(x, 0) = 4 \tan^{-1} \exp \left[\frac{x - x_0}{\sqrt{1 - v^2}} \right], \quad (53)$$

and its time derivative (at $t = 0$):

$$\partial_t u(x, 0) = -2 \frac{v}{\sqrt{1 - v^2}} \operatorname{sech} \left[\frac{x - x_0}{\sqrt{1 - v^2}} \right]. \quad (54)$$

We apply the explicit energy conserving scheme (40) using the following parameters set: space interval $L = 10$, space discretization step $\Delta x = 0.02$, time step $\Delta t = 0.0002$ and velocity of the kink $v = 0.9$ and its center position $x_0 = 5$.

In Fig. 1 the evolution of a kink on the space interval $[0, 10]$ with TBCs of the third order approximation is presented. The corresponding energy evolution is plotted in Fig. 2 using its discrete analogue given by (42). From this plot one can observe that the total energy vanishes with the transition of the wave function through the artificial boundary, which implies that a kink completely leaves the interval $[0, L]$ without reflection at the boundary. For further analyses

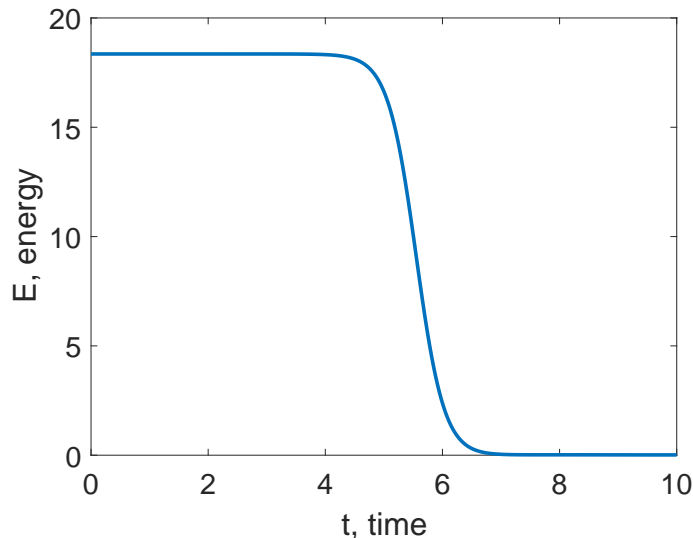


FIG. 2: Time evolution of the discrete kink energy (42) in the interior domain $[0, L]$.

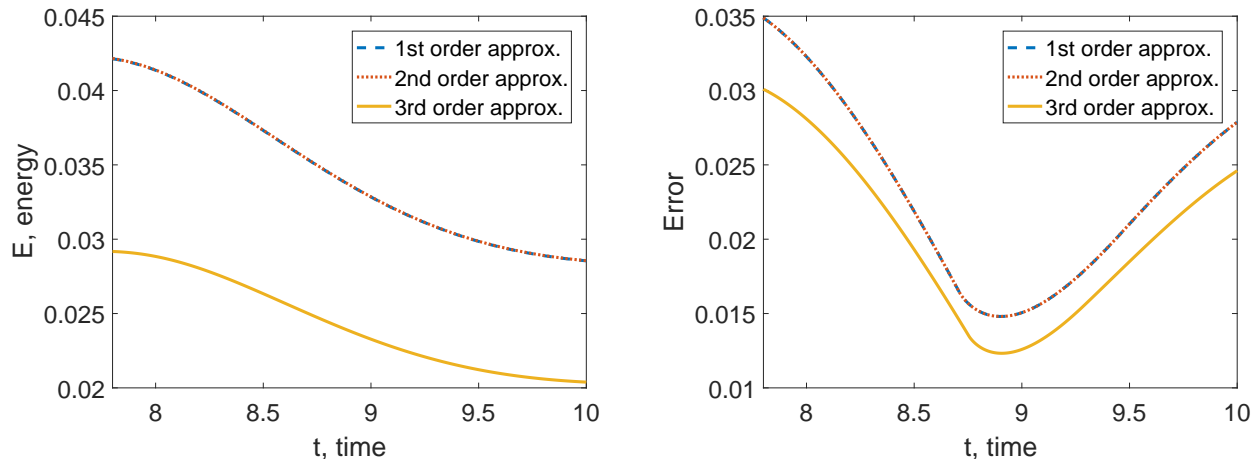


FIG. 3: Comparison of total energies (left panel) and total error (right panel) calculated for the first, second and third order approximations within the last considered time period.

we consider three time intervals of the dynamics: $[0, 3]$ – period, during which no influence of TBCs is observed; $(3, 7.8]$ – within this period the kink passes through the artificial boundary; $(7.8, 10]$ – time left after the kink’s transition.

As the energy must vanish after the kink passes the artificial boundary (i.e. for the third time interval), in Fig. 3 in the left panel it is shown that the energy decreases with higher order TBCs. This can also be checked by computing the error defined as

$$\text{ER}(n\Delta t) = \frac{1}{J-1} \sum_{j=1}^{J-1} |u_j^n|. \quad (55)$$

In Fig. 3 in the right panel one can observe that the error decreases with higher order TBCs. In our numerical investigations we further check the variations in the discrete momentum (7)

$$P^{n+1} = -h \sum_{j \in \mathbb{Z}} (D_k^0 u_j^{n+1})(D_h^0 u_j^n) = -h \sum_{j \in \mathbb{Z}} \frac{u_j^{n+2} - u_j^n}{2k} \frac{u_{j+1}^{n+1} - u_{j-1}^{n+1}}{2h}. \quad (56)$$

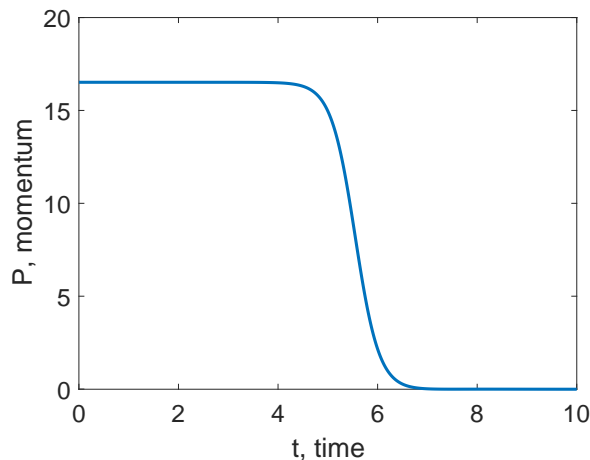


FIG. 4: Time evolution of the discrete momentum (56) in $[0, L]$

Time evolution of the discrete momentum is shown in Fig. 4. This plot demonstrates the same behaviour as that for the energy, which implies reflectionless transmission of a kink-soliton through the artificial boundary.

V. CONCLUSIONS

We have derived explicit transparent boundary conditions for the sine-Gordon equation on a real line. The so-called potential approach is used for reducing the sine-Gordon equation to the linear Klein-Gordon equation. An effective and stable discretization for transparent boundary conditions is proposed and implemented to model the reflectionless propagation of sine-Gordon solitons on a line. A stability analysis and error estimates for the numerical method are provided. The above results can be directly used for modeling the transport of sine-Gordon solitons in a broad variety of physical systems and processes, such as Josephson junctions, deformation propagation in solids, energy transport in DNA and seismic waves in tectonic plates. Although the above treatment deals with the kink solitons, similar approach can be applied for other travelling wave solutions of sine-Gordon equation.

In future work we will extend our approach to two dimensions. Also, we will consider discrete TBCs that are designed directly for the considered numerical scheme. Finally we will transfer our TBCs for sine-Gordon equations on metric graphs, that are needed at the branching points, as it was done for the nonlinear Schrödinger equation in [35].

-
- [1] J. Cuevas-Maraver, P.G. Kevrekidis and F. Williams (Eds.), *The sine-Gordon model and its applications: from Pendula and Josephson junctions to gravity and high-energy Physics*. (Springer International Publishing, 2014).
 - [2] O. Braun and Yu. Kivshar, *The Frenkel-Kontorova Model*, (Springer, 2004).
 - [3] P.G. Drazin and R.S. Johnson, *Solitons: an Introduction* (Cambridge University Press, 1989).
 - [4] M. Peyrard and T. Dauxois, *Physique des solitons*, (EDP Sciences, 2004).
 - [5] H. Ibach and H. Lüth, *Festkörperphysik* (Springer, 2009).
 - [6] M.J. Ablowitz and P.A. Clarkson, *Solitons, Nonlinear Evolution Equations and Inverse Scattering*, (Cambridge University Press, 1999).
 - [7] A. Barone and G. Paterno, *Physics and Applications of the Josephson Effect*, (Wiley, New York, 1982).
 - [8] A. Barone, F. Esposito, C.J. Magee, et al., *Theory and applications of the sine-Gordon equation*, *La Rivista del Nuovo Cimento*, **1**, 227 (1971).
 - [9] J. McCann, *Josephson Junction and Superconductivity Research*, (Nova Science Publishers, 2007).
 - [10] N. I. Gershenzon, V. G. Bykov, and G. Bambakidis, *Phys. Rev. E*, **79**, 056601 (2009).
 - [11] V. G. Bykov, *J. Seismol.*, **18**, 497 (2014).
 - [12] S. Yamosa, *Phys. Rev. A*, **27** 2120 (1983).
 - [13] L. V. Yakushevich, *Nonlinear Physics of DNA*, 2nd edition (Wiley-VCH, Weinheim) 2004.
 - [14] D. Giuliano and P. Sodano, *Europhys.Lett.*, **88**, 17012 (2009).
 - [15] D. Giuliano and P. Sodano, *Nucl. Phys. B*, **811**, (FS) 395 (2009).

- [16] D. Giuliano and P. Sodano, Nucl. Phys. B, **837**, (FS) 153 (2010).
- [17] D. Giuliano and P. Sodano, EPL, **103**, 57006 (2013).
- [18] H. Susanto, S. van Gils, A. Doelman, and G. Derks, Physica C. **408**, 579 (2004).
- [19] H. Susanto, S. van Gils, A. Doelman, and G. Derks, Phys. Rev. B **69**, 212503 (2004).
- [20] Z. Sobirov, D. Babajanov, D. Matrasulov, K. Nakamura, H. Uecker, , EPL **115** 50002 (2016).
- [21] K. Sabirov, S. Rakhmanov, D. Matrasulov, H. Susanto, Phys. Lett. A **382** 1092 (2018).
- [22] D. Babajanov, H. Matyoqubov and D. Matrasulov, J. Chem. Phys., **149**, 164908 (2018).
- [23] D. Matrasulov, K. Sabirov, D. Babajanov, H. Susanto, EPL, **130** 67002 (2020).
- [24] A. Arnold and M. Ehrhardt, J. Comput. Phys., **145(2)**, 611 (1998).
- [25] M. Ehrhardt, VLSI Design, **9(4)**, 325 (1999).
- [26] M. Ehrhardt and A. Arnold, Riv. di Math. Univ. di Parma, **6(4)**, 57 (2001).
- [27] X. Antoine, Ch. Besse, and S. Descombes, SIAM J. Numer. Anal., **43**, 2272 (2006).
- [28] A. Zisowsky and M. Ehrhardt, Math. and Comput. Modell., **47**, 1264 (2008).
- [29] R. Hammer, W. Pötz, A. Arnold, J. Comput. Phys., **256**, 728 (2014).
- [30] X. Wu, J. Zhang, J. Comput. Math., **29**, 74 (2011).
- [31] M. Schwendt, W. Pötz, Comput. Phys. Commun., **229**, 129 (2018).
- [32] J.R. Yusupov, K.K. Sabirov, M. Ehrhardt and D.U. Matrasulov, Phys. Lett. A, **383**, 2382 (2019).
- [33] J.R. Yusupov, Kh.Sh. Matyokubov, K.K. Sabirov and D.U. Matrasulov, Chem. Phys., **537**, 110861 (2020).
- [34] M.M. Aripov, K.K. Sabirov and J.R. Yusupov, *Nanosystems: physics, chemistry, mathematics*, **10(5)**, pp. 501-602 (2019).
- [35] J.R. Yusupov, K.K. Sabirov, M. Ehrhardt and D.U. Matrasulov, Phys. Rev. E, **100**, 032204 (2019).
- [36] J.R. Yusupov, K.K. Sabirov, Q.U. Asadov, M. Ehrhardt and D.U. Matrasulov, Phys. Rev. E, **101(6)** (2020), 062208.
- [37] M. Cui, Num. Meth. Part. Diff. Eqs., **25(3)**, (2009).
- [38] M. Cui, J. Comput. Appl. Math., **235(3)**, 837 (2010).
- [39] M. Sari and G. Gürarşlan, Commun. Numer. Meth. Engrg., **27(7)**, 1126 (2011).
- [40] A.Q.M. Khaliq, B. Abukhodair, Q. Sheng, M.S. Ismail, Numer. Meth. Part. Diff. Eqs., **16**, 133 (2000).
- [41] G. Ben-Yu, P.J. Pascual, M.J. Rodriguez and L. Vázquez, Appl. Math. Comput. **18(1)**, 1 (1986).
- [42] Z. Fei, L. Vázquez, Appl. Math. Comput., **45**, 17 (1994).
- [43] H. Lai and C. Ma, Phys. Rev. E **84**, 046708 (2011).
- [44] M. Dehghan and A. Shokri, Numer Methods Partial Differential Eq. **24(2)**, 687 (2008).
- [45] X. Antoine, E. Lorin, Q. Tang, Mol. Phys., **115**, 1861 (2017).
- [46] J. Zhang, Z. Xu, X. Wu, Phys. Rev. E, **79**, 046711 (2009).
- [47] C. Zheng, SIAM J. Sci. Comput., **29(6)**, 2494 (2007).
- [48] X. Antoine, A. Arnold, C. Besse, M. Ehrhardt and A. Schädle, Commun. Comput. Phys., **4(4)**, 729 (2008).
- [49] M. Ehrhardt, Acta Acustica united with Acustica, **88**, 711 (2002).
- [50] A. Arnold, M. Ehrhardt and I. Sofronov, Commun. Math. Sci., **1(3)**, 501 (2003).
- [51] S. Jiang and L. Greengard, Comput. Math. Appl., **47**, 955 (2004).
- [52] M. Ehrhardt, Appl. Numer. Math. **58(5)**, 660 (2008).
- [53] L. Šumichrast and M. Ehrhardt, J. Electr. Engineering, **60(2)**, 301 (2009).
- [54] X. Antoine et al., J. Comput. Phys., **228(2)**, 312 (2009).
- [55] M. Ehrhardt, Numer. Math.: Theor. Meth. Appl., **3(3)**, 295 (2010).
- [56] P. Klein, X. Antoine, C. Besse and M. Ehrhardt, Commun. Comput. Phys., **10(5)**, 1280 (2011).
- [57] A. Arnold, M. Ehrhardt, M. Schulte and I. Sofronov, Commun. Math. Sci., **10(3)**, 889 (2012).
- [58] R.M. Feshchenko and A.V. Popov, Phys. Rev. E, **88**, 053308 (2013).
- [59] X. Antoine et al., J. Comput. Phys., **277**, 268 (2014).
- [60] M. Taylor, *Pseudo Differential Operators*, Springer, 1974.
- [61] L. Vu-Quoc and S. Li, Comput. Methods Appl. Mech. Engrg., **107**, 341 (1993).
- [62] S. Li and L. Vu-Quoc, SIAM J. Numer. Anal., **32(6)**, 1839 (1995).